Title

Cell-free production of a functional oligomeric form of a Chlamydia major outer-membrane protein (MOMP) for vaccine development

Journal

Journal of Biological Chemistry, 292(36)

ISSN

0021-9258

Authors

He, Wei

Felderman, Martina

Evans, Angela C

et al.

Publication Date

2017-09-01

DOI

10.1074/jbc.m117.784561

Cell-free production of a functional oligomeric form of a *Chlamydia* major outer-membrane protein (MOMP) for vaccine development

Received for publication, March 3, 2017, and in revised form, July 13, 2017 Published, Papers in Press, July 24, 2017, DOI 10.1074/jbc.M117.784561

Wei He[‡], Martina Felderman[§], Angela C. Evans[‡], Jia Geng[‡¶], David Homan[‡], Feliza Bourguet[‡], Nicholas O. Fischer[‡], Yuanpei Li[‖], Kit S. Lam[‖], Aleksandr Noy[‡¶], Li Xing[**], R. Holland Cheng[**], Amy Rasley[‡], Craig D. Blanchette[‡], Kurt Kamrud[§], Nathaniel Wang[§], Heather Gouvis[§], Todd C. Peterson[§], Bolyn Hubby[§], and Matthew A. Coleman[‡ ‡‡1]

From the [‡]Lawrence Livermore National Laboratory, Livermore, California 94550, [§]Synthetic Genomics Vaccine Inc., La Jolla, California 92037, [¶]School of Natural Sciences, University of California, Merced, California 95343, the [‖]Department of Biochemistry and Molecular Medicine and [‡‡]Radiation Oncology, School of Medicine, University of California Davis, Sacramento, California 95817, and the [**]Department of Molecular and Cellular Biology, University of California, Davis, California 95618

Edited by Peter Cresswell

Chlamydia is a prevalent sexually transmitted disease that infects more than 100 million people worldwide. Although most individuals infected with *Chlamydia trachomatis* are initially asymptomatic, symptoms can arise if left undiagnosed. Long-term infection can result in debilitating conditions such as pelvic inflammatory disease, infertility, and blindness. *Chlamydia* infection, therefore, constitutes a significant public health threat, underscoring the need for a *Chlamydia*-specific vaccine. *Chlamydia* strains express a major outer-membrane protein (MOMP) that has been shown to be an effective vaccine antigen. However, approaches to produce a functional recombinant MOMP protein for vaccine development are limited by poor solubility, low yield, and protein misfolding. Here, we used an *Escherichia coli*-based cell-free system to express a MOMP protein from the mouse-specific species *Chlamydia muridarum* (MoPn-MOMP or mMOMP). The codon-optimized mMOMP gene was co-translated with Δ49apolipoprotein A1 (Δ49ApoA1), a truncated version of mouse ApoA1 in which the N-terminal 49 amino acids were removed. This co-translation process produced mMOMP supported within a telodendrimer nanolipoprotein particle (mMOMP–tNLP). The cell-free expressed mMOMP–tNLPs contain mMOMP multimers similar to the native MOMP protein. This cell-free process produced on average 1.5 mg of purified, water-soluble mMOMP–tNLP complex in a 1-ml cell-free reaction. The mMOMP–tNLP particle also accommodated the co-localization of CpG oligodeoxynucleotide 1826, a single-stranded synthetic DNA adjuvant, eliciting an enhanced humoral immune response in vaccinated mice. Using our mMOMP–tNLP formulation, we demonstrate a unique approach to solubilizing and administering membrane-bound proteins for future vaccine development. This method can be applied to other previously difficult-to-obtain antigens while maintaining full functionality and immunogenicity.

Chlamydia trachomatis, a sexually transmitted Gram-negative bacterium that infects both men and women, is the most common sexually transmitted infection (STI)[2] worldwide (1). After invading eukaryotic cells, *Chlamydia* replicate within endosomal inclusions. Their life cycles begin with a metabolically inactive infectious form called the elementary body (EB) that measures ~300 nm in diameter. In this form, up to 75% of the rigid outer-membrane surface of EB is coated with a porin protein called major outer-membrane protein (MOMP). After the EB is endocytosed, it differentiates into the reticulate body, a metabolically active form that measures ~1,000 nm in diameter (2–4). After 48 h, active reticulate bodies revert back to an inactive EB state and are released from the host cell. Surrounding cells are then infected with EBs, and the infectious life cycle repeats itself (2).

Although *Chlamydia* infections are treatable, the majority of infected individuals are asymptomatic, and permanent health damage can occur when the infection is left undiagnosed for a long period of time. For example, certain types of *Chlamydia trachomatis* can cause trachoma, an infection of the eye prevalent in Africa that may lead to blindness. Other infections can lead to pelvic inflammatory disease, ectopic pregnancy, and neonatal pneumonia. Although drugs to treat *Chlamydia* exist, reoccurrence of infection remains problematic. The potential

This work was supported by United States Department of Energy Contract DE-AC52-07NA27344; NCI, National Institutes of Health Grants R01CA115483 and R01CA199668; and NIAID, National Institutes of Health Grant R21 RAI120925A. M. Felderman, K. Kamrud, N. Wang, H. Gouvis, T. C. Peterson, and B. Hubby are employed by Synthetic Genomics Vaccine Inc. Synthetic Genomics Vaccine Inc. (La Jolla, CA) provided funding under a Work for Others Agreement to Lawrence Livermore National Laboratory. As a funding agency they had no role in study design or data collection and analysis for publication of the data. They do have a financial interest through the development of novel synthetic biology strategies for vaccine development. This does not alter the authors' adherence to all the JBC policies on sharing data and materials. The content is solely the responsibility of the authors and does not necessarily represent the official views of the National Institutes of Health.

This article contains supplemental Figs. 1–5.

[1] To whom correspondence should be addressed: Lawrence Livermore National Laboratory, 7000 East Ave., Livermore, CA 94550-7133. Tel.: 925-423-7687; Fax: 925-424-3130; E-mail: coleman16@llnl.gov.

[2] The abbreviations used are: STI, sexually transmitted infection; MOMP, major outer-membrane protein; EB, elementary body; mMOMP, *Chlamydia muridarum* MOMP; tNLP, telodendrimer nanolipoprotein particle; NLP, nanolipoprotein particle; CA, cholic acid; DLS, dynamic light scattering; SEC, size exclusion chromatography; DMPC, 1,2-dimyristoyl-sn-glycero-3-phosphorylcholine; VD1, first variable domain/loop; Bis-Tris, 2-[bis(2-hydroxyethyl) amino]-2-(hydroxymethyl)propane-1,3-diol; CryoEM, cryo-electron microscopy.

severity of *Chlamydia* infection, even when asymptomatic, highlights the need for a long-term protective vaccine.

Epidemiological data, animal models, and early vaccine trials using an inactivated strain of bacteria against trachoma have demonstrated serotype/serogroup-specific immunity to the 15 known serovars of *C. trachomatis.* However, immunity is short-lived and typically declines in 1–2 years. It is believed that prolonged immunity is related to serotype-specific antigens like MOMP (5). Experimental MOMP vaccines based on denatured or non-native recombinant preparations yielded only partial protection in a mouse model using *Chlamydia muridarum* (previously called *C. trachomatis* mouse pneumonitis) (6–9). Although sterilizing immunity elicited by any recombinant MOMP or chimeric epitopes has not been demonstrated, a preparation consisting of the native MOMP isolated directly from mammalian cells infected with *C. muridarum* has been shown to elicit robust humoral and cell-mediated immune responses and protects against infection and infertility (8). This protection is believed to be dependent on the presence of a distinctive trimer state of the native MOMP protein (6, 7, 9). However, the process of extracting native MOMP from *C. trachomatis* is laborious and difficult to produce for large-scale commercial applications. Thus, the development of a *Chlamydia* vaccine based on MOMP requires a recombinant expression approach that maintains MOMP in its functional state and can be easily commercialized.

Extensive efforts to express MOMP in bacterial systems have yielded poor results due to incorrect MOMP protein folding (10–12). MOMP is a complex protein that comprises 16 transmembrane domains, rendering it difficult to recombinantly synthesize in a correctly folded state. Recently, Wen *et al.* (13) expressed *C. trachomatis* MOMP on *Escherichia coli* outer membrane and demonstrated improved protein folding and immunogenicity. However, in that study, they had to alter the gene sequence to achieve the targeted expression. In addition, the method also involved strenuous detergent extraction and a lengthy process of protein purification.

Cell-free methods are ideal for production of protein antigens that are hard to produce with traditional methods. Other groups have used cell-free methods to express membrane proteins and have successfully incorporated membrane proteins into proteoliposomes. For example, Takeda *et al.* (14) used cell-free methods combined with liposome technology to produce membrane-bound antigens for vaccination. However, proteoliposome formation requires multiple reconstitution steps over a lengthy period of time and may not allow for native oligomerization (15, 16). It also remains a problem that the membrane proteins embedded in liposomes may have only one end exposed to the environment, and it is difficult to control the correct orientation. Newer methods are required to facilitate expression, folding, and solubilization of a membrane protein such as MOMP that forms trimers with many transmembrane helices. In this study, we introduce telodendrimer nanolipoprotein particles (tNLPs) as a vehicle to solubilize and maintain mMOMP protein in its functional state using a cell-free expression system.

Nanolipoprotein particles (NLPs) are 6–20-nm disc-shaped particles formed by the spontaneous self-assembly of phospholipids and scaffold apolipoproteins. NLPs are analogous to high-density lipoproteins (HDLs), particles naturally involved in mammalian lipid metabolism (17–21). These NLPs have been shown to support functional membrane proteins and provide an excellent alternative to traditional lipid-based platforms (*e.g.* liposomes) for vaccine delivery. The procedure of NLP synthesis is very flexible as lipid and protein components can be easily substituted to accommodate various membrane proteins or achieve desired chemical properties (22–24). NLPs also enhance membrane protein solubility and *in vivo* delivery (25). Several groups, including our team, have successfully reconstituted a variety of membrane proteins, including rhodopsins, G-protein–coupled receptors, cytochrome P450, and functional channels, using NLPs (26–36). We have also developed a variety of approaches for conjugating many different compounds to the NLP platform (37–39) and have successfully assembled NLPs containing a range of different adjuvants, including monophosphoryl lipid A and CpG oligodeoxynucleotides (40, 41). Furthermore, the NLP platform was shown to display no toxicity both *in vitro* and *in vivo* even when administered at high doses (39). Recently, we developed a class of NLPs that incorporates telodendrimers, cholic acid-based amphiphilic polymers comprising dendritic oligomers of cholic acids and a linear polyethylene glycol (PEG) tail (42). This class of telodendrimer-additive NLPs is called tNLPs (24). Here, we used a telodendrimer with a 5,000-dalton PEG tail and eight cholic acid headgroups (PEG^{5000}-CA_8). The specific type of telodendrimer was chosen based on our previous experiments where we learned that the use of telodendrimer PEG^{5000}-CA_8 generates stable NLPs with low aggregation and an ideal size (~25 nm) for supporting membrane proteins like MOMP. We are able to change the ratio of telodendrimer to lipid to control the homogeneity of the tNLP where ~1% telodendrimer generates mostly homogeneous tNLPs. Telodendrimer addition improves NLP monodispersity and allows the formation of larger sized tNLP particles, which may potentially accommodate membrane protein multimers (24).

In the current study, we used the tNLP technology to produce functional mMOMP. This mMOMP expression is coupled with tNLP synthesis in an *E. coli*-based cell-free expression system, resulting in the robust production of functional mMOMP–tNLP complexes. Quality analysis of the synthesis of tNLP complexes included SDS-PAGE, Western blotting with epitope-specific antibodies, functional assessment, dynamic light scattering (DLS), transmission electron microscopy, and size exclusion chromatography (SEC). Characterization of the assembly product demonstrated that mMOMP is incorporated in the tNLP and that it can form oligomeric structures while remaining soluble and free from aggregation. The cell-free tNLP method eliminates the need to overexpress insoluble mMOMP protein in cells or to reconstitute mMOMP with detergent (32, 43). In a mouse immunization study, mMOMP–tNLPs adjuvanted with CpG oligodeoxynucleotide 1826 elicited a strong antigen-specific IgG response. These findings demonstrate that mMOMP–tNLP is a strong candidate for recombinant *Chlamydia* vaccine development. Our cell-free expression approach, coupled with *in situ* tNLP assembly, provides a robust model system for expressing difficult-to-obtain

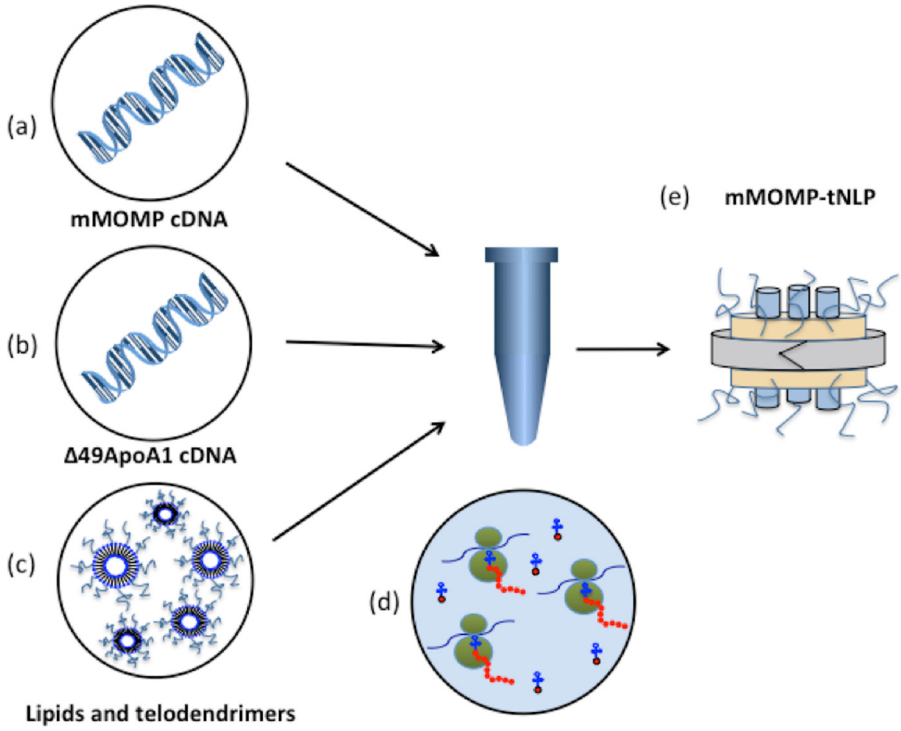

Figure 1. mMOMP–tNLP preparation. *a–c*, mMOMP DNA, Δ49ApoA1 DNA, and DMPC/telodendrimer were mixed in a cell-free reaction chamber. *d*, protein translation and the self-assembly of mMOMP–tNLPs in a cell-free lysate. *e*, the assembled mMOMP–tNLP product is shown.

target membrane proteins amenable for formulation in the next generation of multivalent subunit vaccines.

Results

Cell-free co-translation supports soluble mMOMP expression

Codon optimization was used to alter sequences for mMOMP–tNLP expression in *E. coli* cell-free lysates (Fig. 1). Codon optimization of the Δ49ApoA1 and mMOMP sequences resulted in a ~20% change in the primary protein coding sequences for both proteins (Fig. 2). Co-translation reaction conditions using plasmids encoding Δ49ApoA1 and mMOMP were initially screened using a BODIPY-lysine fluorescent amino acid to simplify visualization of protein expression and solubility screening. The BODIPY-lysine fluorescent amino acid is randomly inserted at lysine positions within the protein at a low insertion rate. Increasing the Δ49ApoA1 plasmid in the reaction will subsequently decrease the mMOMP expression in the cell-free reaction (supplemental Fig. 1). Within the 5-fold difference in ApoA1 plasmid, the protein expression levels are expected to vary proportionally to the plasmid input. Meanwhile, the expression level of mMOMP decreases proportionally. The mMOMP protein is highly hydrophobic and is normally insoluble in the absence of a native lipid bilayer or detergents. Co-translation with both mMOMP and Δ49ApoA1 plasmids in the presence of DMPC lipid alone did not result in a soluble mMOMP expression product with only about 10% solubility of mMOMP. Expression of mMOMP in the presence of DMPC and telodendrimer PEG^{5000}-CA_8 but without apolipoprotein Δ49ApoA1 also resulted in less than 10% mMOMP solubility. Soluble mMOMP was only observed when mMOMP and Δ49ApoA1 were co-translated in the presence of both DMPC lipid and telodendrimer PEG^{5000}-CA_8. The solubility of mMOMP increased from 10 to 75% upon insertion into the tNLP (supplemental Fig. 2).

Reactions were scaled up to 1 ml to produce sufficient quantities of MOMP for subsequent nickel purification utilizing the His tag present on the apolipoprotein scaffold component of the tNLP. The small amount of mMOMP that is solubilized by telodendrimer micelle is removed during nickel affinity purification because there is no His tag present on the mMOMP. The purification provided a complex that was >95% pure based on SDS-PAGE analysis. On average, a 1-ml reaction yielded 1.5 mg of purified mMOMP–tNLP complex (Fig. 3*a*) based on total protein quantitation (the 1.5 mg represents total protein MOMP + NLP). Distinct bands indicated that the two proteins, Δ49ApoA1 and mMOMP, were co-purified as a complex. Because our mMOMP protein does not have a His tag, this indicates that mMOMP must be associated with the tNLP. To further characterize the mMOMP–tNLP complex, individual affinity purification elution fractions were assessed by SEC (Fig. 3*b*). SEC analysis confirmed that each mMOMP–tNLP fraction eluted at the appropriate time (retention time, ~7 min) without free proteins or lipid aggregates (retention time, ~9 and 5 min, respectively), indicating that the complex was a homogenous mixture of mMOMP–tNLPs (supplemental Fig. 3). Dot blots of an SEC peak fraction probed with mAb-His and mAb40, a monoclonal antibody that recognizes a linear epitope on the first variable domain/loop (VD1) of the mMOMP protein, demonstrated that both Δ49ApoA1 and mMOMP were co-localized (Fig. 3*c*).

mMOMP–tNLPs form disc-shaped nanoparticles

Dynamic light scattering was used to visualize the overall size of the purified mMOMP–tNLP complex. The empty tNLPs

Figure 2. Codon-optimized sequences. DNA sequences of Δ49ApoA1 (*a*) and mMOMP (*b*) proteins are shown with nucleotide alterations in *white* background. All mutations are silent mutations.

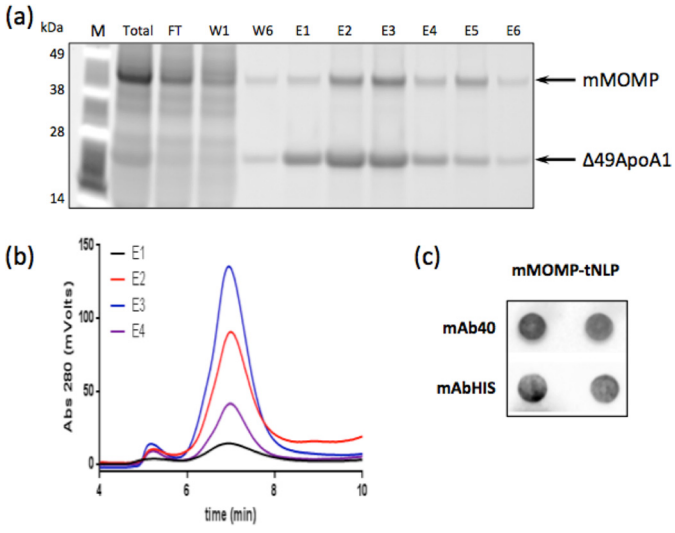

Figure 3. Expression and purification of mMOMP–tNLP. *a*, SYPRO Ruby protein gel stain of 4–12% SDS-PAGE of affinity-purified mMOMP–tNLP. Total cell-free lysate (*Total*), flow-through (*FT*), Washes 1 and 6 (*W1* and *W6*), and Elutions 1 through 6 (*E1–E6*) are shown. All samples were boiled for 5 min in the presence of 50 mM DTT. mMOMP is at 40 kDa, and the Δ49ApoA1 is at 22 kDa. *M*, molecular mass marker. *b*, SEC traces of mMOMP–tNLP particles. Different elutions still maintain the same sized mMOMP–tNLPs. *c*, dot blot of mMOMP–tNLP sample (SEC peak fraction using the nickel affinity purified elution *E2* as input) in duplicate probed with mAb40 and mAb-His.

were ~10 nm in diameter (Fig. 4*a*). The mMOMP–tNLP particle sizes showed an almost 4-fold increase in diameter to about 40 nm (Fig. 4*b*). This large increase was unexpected but plausible given that each mMOMP contains 16 transmembrane domains. In addition, image analysis using cryo-electron microscopy (cryoEM) indicated that mMOMP–tNLPs were disc-shaped (Fig. 4*c*). A comparison between empty tNLPs and mMOMP–tNLPs via cryoEM also confirmed the larger particle size of mMOMP–tNLPs. The cryoEM images also revealed that mMOMP–tNLPs, not empty tNLPs, contained multiple regions of enhanced density. Because there are no fixation or dehydration steps during cryoEM, the density presented is directly proportional to the charge density of the proteins and lipids. All tNLPs have a well defined high-density outer rim corresponding to the scaffold protein. Empty tNLPs display low density inside the disc, whereas mMOMP–tNLPs illustrate high-density regions within the mMOMP–tNLP. These high-density regions likely represent mMOMP pores formed inside the mMOMP–tNLP. These results were similar to previously reported Bax-mediated pore formation inside a nanodisc (44). Interestingly, although the resolution of the EM image does not allow for further analysis, we were able to see many mMOMP–tNLP particles that contained two to four high-density regions indicative of multiple mMOMP proteins inserted into a single mMOMP–tNLP.

mMOMP associated with tNLPs forms higher order structures

Membrane-bound porins are known to be resistant to denaturant, providing a means to identify the formation of oligomer species using SDS-polyacrylamide gels (45, 46). By analyzing mMOMP–tNLP in the presence and absence of both heat and

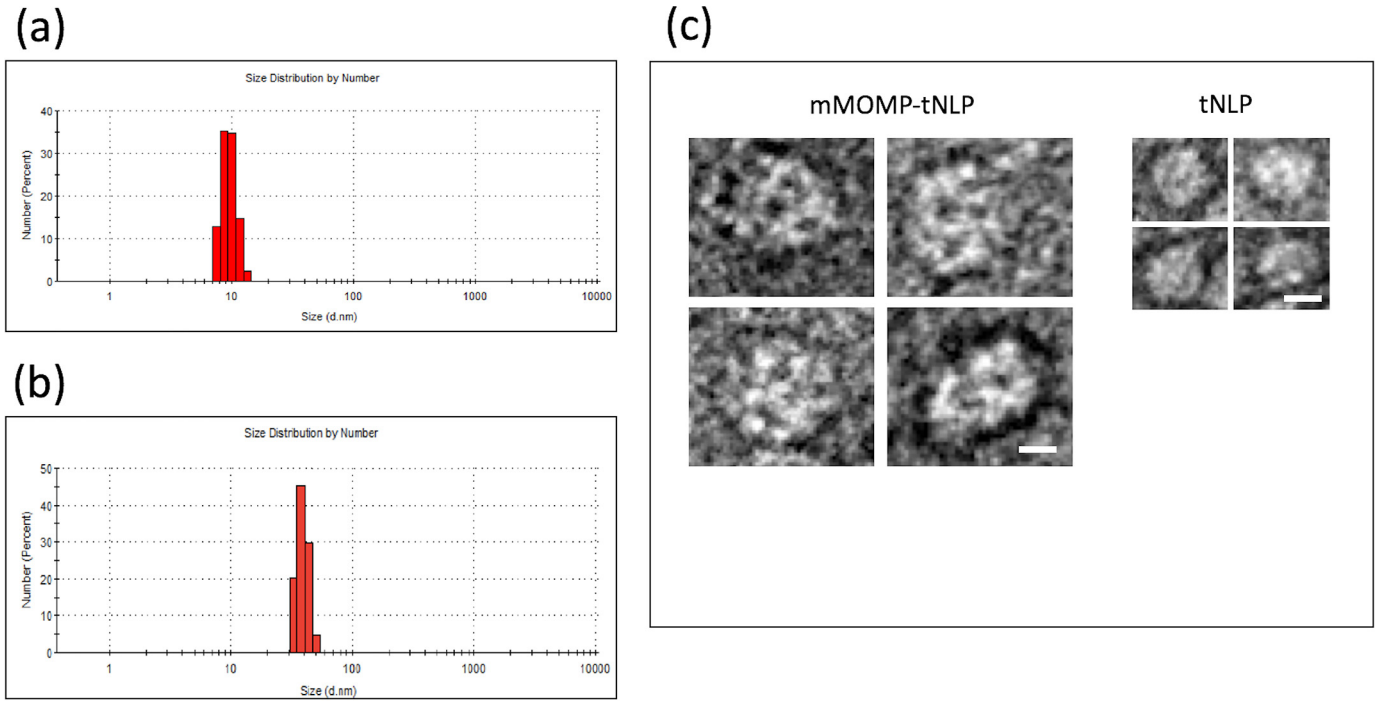

Figure 4. mMOMP insertion increases the size of tNLPs. *a*, the size distribution of empty tNLPs as measured by DLS. *b*, the size distribution of mMOMP–tNLPs measured by DLS. *c*, cryoEM demonstrates that the mMOMP particles are disc-like in shape and that there are size differences between tNLP and mMOMP–tNLP particles. High-density areas can be seen in the images of mMOMP–tNLPs, indicating pore formation. *Scale bars*, 10 nm.

reducing agent, higher order oligomers of mMOMP were identified. SDS-PAGE of heated samples in the presence of DTT showed primarily two distinct bands on the gel, corresponding to mMOMP and Δ49ApoA1 at ~40 and 22 kDa, respectively. However, with heat and reducing agent (DTT) removed, distinct bands corresponding to mMOMP oligomers were observed on the gel that were absent in tNLP-alone control, indicating that these oligomers are part of mMOMP and not oligomers of the apolipoprotein scaffold (Fig. 5*a*). These results closely resemble the gel banding pattern attributed to oligomer formation of native MOMP (45). Western blot analysis probing with mAb40, a monoclonal antibody that recognizes a linear epitope on VD1 of the MOMP protein, also indicated the formation of the higher order structures of mMOMP (Fig. 5*b*). These multimeric structures are not evident in recombinant MOMP produced in traditional *E. coli* expression systems with the exception of the Wen *et al.* (13) study in which MOMP is target-expressed in the *E. coli* outer membrane. This suggests that the environment in which MOMP sits remains critical for correct protein folding. We believe that in our system the confinement to the constrained lipid bilayer of the tNLP can promote native-like MOMP protein oligomerization (46).

Dot blots were then tested to determine whether adding both heat and reducing agent affects mMOMP antibody binding. Antibodies specific for mMOMP linear epitope detection (mAb40) with and without heat and reducing agent resulted in the same intensity of signal, indicating that heat and DTT do not affect the mAb40 binding to mMOMP. As a control, mAb-His was always able to detect the apolipoprotein supporting scaffold (supplemental Fig. 4).

tNLP-solubilized mMOMP forms functional pores in bilayers

Previous studies have shown that the presence of mMOMP initiates pores in lipid bilayers (10). Therefore, we used conductance analysis to test the function of mMOMP supported in the tNLP. The pore-forming activities of mMOMP–tNLP were tested in a typical black lipid membrane channel reconstitution experiment using the single-channel recording technique (47). In brief, the conductance assay measured the change in the current going through the lipid bilayer as the protein pores were inserted into it with each insertion producing a stepwise increase in the current. Discrete increases in current were observed 3–5 s after the addition of mMOMP–tNLP solution to the *cis*-chamber. This current increase corresponded to the bilayer pore formation by the mMOMP proteins, indicating functional mMOMP insertion (Fig. 6*a*, traces *ii–iv*). Control experiments with tNLP alone did not produce channel activity under a series of applied transmembrane voltages ranging from −100 to +100 mV (Fig. 6*a*, trace *i*). To analyze this assay, we converted the magnitude of the current step into conductance increase values (which are independent of the applied voltage). The mMOMP–tNLP conductance was predominantly ~172 picosiemens at physiological condition. The individual conductance steps collected from a large number of incorporation events from multiple experimental traces were then plotted on a histogram (Fig. 6*b*). The fusion of an NLP to a membrane bilayer has been studied recently (48). We assume that mMOMP–tNLPs fused to a bilayer in a similar fashion where mMOMP is inserted into the bilayer during the fusion and the NLP scaffold stays attached to the bilayer. If the protein does not oligomerize in the membrane, we would expect the histogram to include conductance peaks at 1×, 2×, 3×, etc. multi-

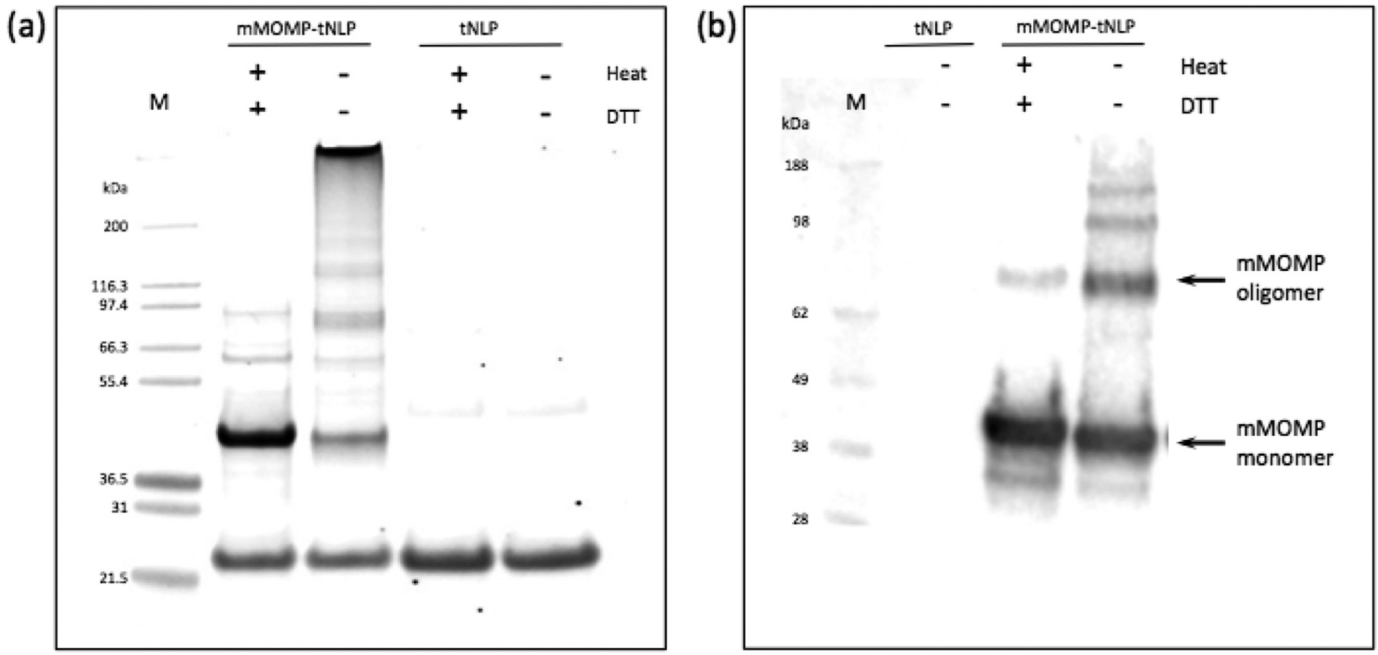

Figure 5. mMOMP forms higher order structures in mMOMP–tNLPs by SDS-PAGE and Western blotting. *a*, SYPRO Ruby protein gel stain of 4–12% SDS-PAGE of affinity-purified mMOMP–tNLP and tNLP alone. mMOMP monomer shows a band at ~40 kDa, and the Δ49ApoA1 shows a band at 22 kDa. The mass ratio of soluble mMOMP to apolipoprotein is ~2:1 as determined through densitometry analysis. In *lane 2*, heat and reducing agent break down higher order mMOMP structure. In *lane 3*, the presence of higher order bands indicates mMOMP multimer conformation. *b*, Western blot of mMOMP–tNLP and tNLP alone. Shown is a transfer membrane probed with mAb40 (1:1,000 dilution). As indicated, samples were incubated at room temperature or boiled for 5 min in the presence of 50 mM DTT. *M*, molecular mass marker.

ples of the value of the conductance of the individual mMOMP protein. The histogram fits well with two distinct peaks that correspond to 1× and 3× multiples of the individual protein conductance. The 1× and 3× multiples of a single conductance value suggest that mMOMP inserts into the mMOMP–tNLP as a mMOMP monomer (1×) or as a mMOMP trimer (3×). Interestingly, attempts to fit the histogram to three peaks at 1×, 2×, and 3× multiples did not produce a better fit than just two peaks. Thus, we conclude that mMOMP protein inserts into the tNLP bilayer membrane as a monomer or as a trimer (not as a dimer).

The mMOMP–tNLP complex elicits an IgG response in mice

The tNLPs (negative control) and mMOMP–tNLPs were adjuvanted with CpG and injected intramuscularly into mice. Other groups were injected with either PBS (negative control) or *Chlamydia* EB (positive control). We found that mMOMP–tNLP supports the addition of CpG adjuvant and elicits significant levels of antigen-specific antibody titers compared with CpG–tNLP (no antigen) and PBS controls (Fig. 7*a*). Pooled mouse sera from injected mice were then probed by Western blotting to detect specific mMOMP binding (Fig. 7*b*). The sera from mice injected with mMOMP–CpG–tNLP showed strong mMOMP binding. The lane with sera immunized with *Chlamydia* EB also showed some mMOMP binding. It is not surprising that EB sera showed less binding than mMOMP–CpG–tNLP sera because EB contains many other proteins other than mMOMP. Therefore, there were many antibodies generated against EB, and only a portion of these antibodies was mMOMP-specific. Sera from PBS and CpG–tNLP control groups showed no mMOMP binding.

Discussion

Chlamydia is the most commonly reported sexually transmitted infection worldwide. There is a need to decrease its prevalence and to reduce associated diseases caused by long-term infection. Reducing one's exposure to *Chlamydia* can occur through safe sex measures, frequent STI screening, and partner communication. Although antibiotics are administered to treat *Chlamydia* infections, early screening and diagnosis are key to preventing complications associated with long-term, untreated infections. It is also worth noting that individuals on antibiotic treatment are more prone to reinfection (1, 2). Given the potential shortcomings of antibiotic treatment and the reliance on screenings for early detection of *Chlamydia* infection, the search for optimal antigens as a vaccine can decrease the prevalence of infection worldwide and prevent long-term pathological damage.

Inactivated *Chlamydia* EB has been tested as a vaccine and does display a degree of protection in mouse models (49). However, this type of protection is often serovar-specific. Moreover, vaccination with live *Chlamydia* EB or whole *Chlamydia* bacteria brings with it obvious safety concerns. Due to the risk associated with live pathogen vaccines, a highly immunogenic MOMP antigen from *Chlamydia* is considered a viable and safer candidate antigen for a vaccine. MOMP comprises about 60% of the outer-membrane protein of *Chlamydia* bacteria (50), and it can elicit both neutralizing antibody and cell-mediated immune responses critical for disease resolution (51). Previous studies using recombinant MOMP expressed in *E. coli* were not entirely effective in eliciting an immunogenic response, which may be due to a lack of MOMP native confor-

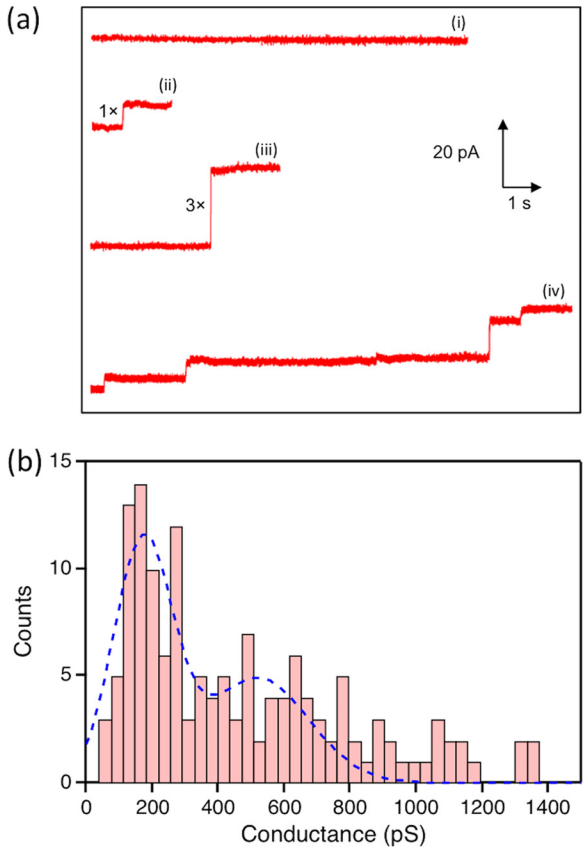

Figure 6. mMOMP–tNLPs initiate pore-forming channels. *a*, conductance traces recorded at 50-mV applied voltage in physiological conditions after tNLP alone (trace *i*) and mMOMP–tNLPs (traces *ii–iv*) were added to the measurement chamber. Current increases seen after mMOMP–tNLP addition indicate pore formation. Representative traces show 1× (trace *ii*) and 3× (trace *iii*) mMOMP–tNLP incorporations. Trace *iv* shows several incorporations events occurring in quick succession. *b*, histogram of 184 conductance events. The *dashed line* indicates the best fit to a sum of Gaussian peaks for 1× and 3× incorporation events. *pS*, picosiemens.

mation such as oligomer formation (12, 46). It is noteworthy that in a recent study, Wen *et al.* (13) were able to express recombinant MOMP on *E. coli* outer membrane that allowed for native-like oligomer formation. They further demonstrated that the oligomer formation is critical for effective immunogenicity (13). However, this recombinant MOMP requires detergent solubilization and a lengthy purification procedure. Moreover, Wen *et al.* (13) did not demonstrate specific immunity to mouse-specific chlamydia, *C. muridarum*.

NLPs hold great potential as vaccine delivery vehicles for membrane-bound antigens such as MOMP. They can be easily assembled with various lipids, apolipoproteins, and other additives like immunogenic adjuvants. NLPs also allow access to both the cytoplasmic and extracellular portions of the membrane protein, which may maximize the exposure of the immunogenic epitope. NLPs have been shown to incorporate many different membrane proteins such as receptor tyrosine kinases and several G-protein–coupled receptors (32, 43, 52, 53). In addition, NLPs display no toxicity when administered *in vivo* (39). A previous study has shown that NLP scaffold proteins may cause a minor immunogenic response (39); however, such immunogenicity can be minimized by matching the species of the scaffold protein to the animal model. Recently, the discovery of the tNLP has enabled further control of particle size and reduced aggregation that facilitates the incorporation of membrane protein multimers (24).

When comparing mMOMP–NLPs with mMOMP–tNLPs, we found that NLPs do not solubilize mMOMP as well as the tNLP particles (supplemental Fig. 2). mMOMP protein functions as a porin and is known to form hydrophobic oligomers; therefore, it tends to aggregate (45). Thus, although NLPs provide a soluble environment for mMOMP, they are still prone to aggregate through mMOMP–mMOMP interactions (54, 55). With the addition of telodendrimer, this mMOMP protein aggregation was diminished. We believe that the PEGylated tail of the telodendrimer protects the mMOMP from interacting with surrounding mMOMP–tNLPs and thus increases its solubility. Although not tested in these experiments, PEGylation also may play a role in stabilizing the nanoparticles. Furthermore, in a standard ApoA1-derived NLP, there is an average of two scaffold proteins per NLP. For a telodendrimer NLP with increased size, it is likely that the number of scaffold proteins per NLP remains the same, and the telodendrimer functions as additional "supporting scaffold" to further stabilize the NLP.

It is known that native MOMP forms dimers, trimers, and tetramers in an oxidized environment (10). It has also been demonstrated that maintaining native MOMP structure is necessary to elicit a robust immune response (9, 12, 13). We show through SDS gels without heat and reducing agents that these mMOMPs supported by tNLP particles mimic native mMOMP oligomer structures. Interestingly, the main form of the mMOMP oligomer, although it has the size of a dimer, may actually represent a trimer as has been seen with the native MOMP described in Sun *et al.* (45). In that study, they also found that the property of oligomerization is an important indicator for proper function and effective vaccination. Thus, the oligomer formation is an important part of demonstrating functional relevancy for the mMOMP protein preparation (12). The crystal structure of *Chlamydia* MOMP is not yet solved, but the dimension of the MOMP protein has been reported to be ~3–3.5 nm in diameter (56). Given the size of a tNLP (>25 nm), it is plausible that up to three to four MOMP proteins can fit in a single tNLP.

The cryoEM studies indicate that some amount of our cell-free–expressed mMOMP–tNLP contains multiple mMOMPs. Furthermore, the conductance assay suggests that a population of mMOMP in the mMOMP–tNLP sample is likely to be in a functional oligomeric state in the bilayer. By varying the amount of mMOMP, we saw similar step changes in the level of conductance, indicating that mMOMP was forming consistent open pores and mMOMP was inserted in the membrane. Next we assessed the oligomeric state of mMOMP based on instances of current level changes. The data were collected over 184 independent experimental measurements in which the incorporated channels fuse with the bilayer in what seems like singular or trimeric state. Although we did not specifically design the experiment to study the gating nature of mMOMP opening and closing, the cell-free mMOMP–tNLP seems to have a pore that stays open under the experimental conditions. It should be noted that the gating property of *Chlamydia* MoPn-MOMP is not well documented. In numerous

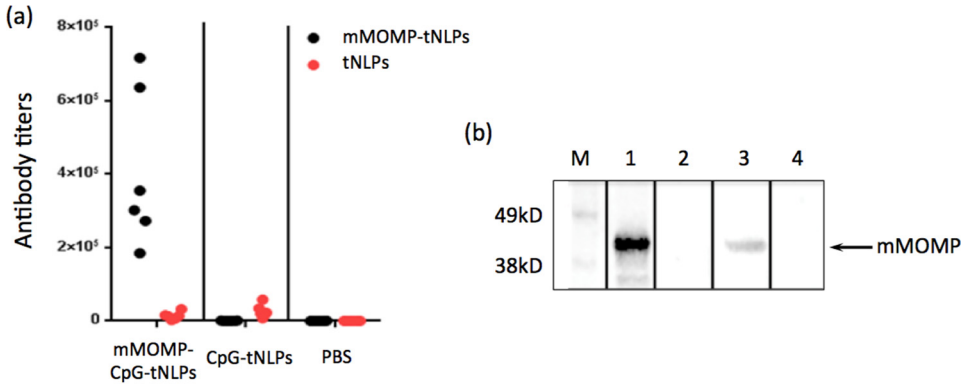

Figure 7. *In vivo* testing with mMOMP–tNLPs. *a*, mMOMP–tNLPs elicit significant antibody titers. Sera from mice immunized with mMOMP–CpG–tNLPs, CpG–tNLPs, and PBS were loaded on ELISA plate precoated with mMOMP–tNLPs (*black dots*) or empty tNLPs (*red dots*), and antibody titers were measured. *b*, four Western blots are shown. The mMOMP protein is loaded onto each lane equally. Mouse sera from the mice immunized with the four different conditions were then incubated with the blot overnight. *Lane 1* is blotted with mouse sera immunized with mMOMP–CpG–tNLP. This blot shows significant mMOMP antibody binding. *Lane 2* is blotted with mouse sera immunized with empty tNLP–CpG. *Lane 3* is blotted with mouse sera immunized with live *Chlamydia* EB. This blot confirms that *Chlamydia* EB induces MOMP antibodies that bind to our recombinant mMOMP. The decreased signal from this blot is because *Chlamydia* EB contains many surface antigens, not just mMOMP; therefore, it induces a large variety of antibodies. *Lane 4* is blotted with mouse sera immunized with PBS control group and shows no mMOMP binding. *M*, molecular mass marker.

studies on other types of MOMP, similar results were observed under similar conditions as described in our present study (57, 58). Accordingly, we hypothesize that our cell-free–produced mMOMP adopted a functional conformation, which has never been reported by any cell-free–based recombinant MOMP. Importantly, we did not need to cross-link the recombinant protein to observe oligomerization. Cell-free expression followed by direct insertion into the tNLP appears to help maintain the functional conformation of membrane-bound proteins (43, 59). The tNLP also provided an ideally sized platform for mMOMP multimer insertion. By altering the plasmid ratios of both mMOMP and ApoA1 in the cell-free mixture, we are able to control the expressed ratios of mMOMP:ApoA1 and control the number of mMOMP per tNLP. The PEG tail of telodendrimer also played a critical role in preventing mMOMP-mediated aggregation, allowing multimer-containing mMOMP–tNLP to stay water-soluble.

It has been reported that native MOMP with trimer structure is the best antigen in inducing protection (60). We believe our mMOMP–tNLP retains functional pores that oligomerize in a similar fashion as native MOMP. Our approach offers a simpler process for generating a potentially effective vaccine as compared with refolded recombinant MOMP proteins using other expression and purification methods. In the current study, cell-free–produced mMOMP–tNLP successfully induced MOMP-specific antibody production. The antisera are able to recognize both the native (Fig. 7*a*) and denatured (Fig. 7*b*) forms of mMOMP–tNLP. Future experiments will include testing whether antisera can effectively recognize live *Chlamydia* EB. It will also be interesting to determine whether the recognition is always against the mMOMP linear epitope or whether it can be conformation-specific. In our experiment, we observed a low level of immune response toward the ApoA1 protein construct used in this study (supplemental Fig. 5). We hypothesize that this low-level response is due to extraneous sequence present in this construct to facilitate affinity purification of the NLP. Furthermore, the reactivity to the construct was only observed in the presence of the CpG adjuvant, indicating low immunogenicity of the NLP construct. In other studies performed by our group, we have not observed detectable antibody production against scaffold proteins that are species-matched and lack affinity or linker sequences.

Conclusion

In this study, we used a cell-free method coupled with tNLP technology to produce a recombinant mMOMP that is soluble and functional. The telodendrimer NLP platform represents a novel method to effectively solubilize membrane proteins with a large number of transmembrane domains. Evidence from SDS-PAGE, cryoEM, and conductance assays indicates functional multimer formation. We demonstrated that immunogenic adjuvants like CpG were easily incorporated into our mMOMP–tNLP formulation. Sera from mice immunized with mMOMP–tNLPs also showed strong antibody titers that cross-reacted with *Chlamydia* EB. Overall, our cell-free–produced mMOMP–tNLPs show great promise for further development as a *Chlamydia* vaccine. Our characterization and high-yield production of mMOMP–tNLPs serve as a model method that can be applied to other difficult-to-obtain antigens. Future work will include immunology studies that analyze the protective ability of mMOMP–tNLPs to fully evaluate their effectiveness as a vaccine.

Experimental procedures

Plasmids

The truncated form of mouse ApoA1 (Δ1–49), or Δ49ApoA1, gene and mMOMP gene were assembled from oligonucleotides and cloned into NdeI/BamHI-digested pIVEX2.4d vector (Roche Molecular Diagnostics) using Gibson Assembly. Briefly, Archetype® software was used to design 60-bp-long, overlapping oligonucleotides covering the DNA sequence of interest (Δ49ApoA1 including 90-bp 5′ and 3′ vector overlap to pIVEX2.4d). The 60-bp oligonucleotides overlapped neighboring oligonucleotides by 30 bp. In addition, forward and reverse primers (distal primers) were designed for amplification of the DNA sequence of interest. The pIVEX2.4d vector cloned with

Δ49ApoA1 contained a His tag used for nickel affinity purification as described previously (52). The plasmid cloned with mMOMP gene does not have a His tag. The codon-optimized gene sequences are shown (Fig. 2).

DMPC/telodendrimer preparation

We have previously published the production and use of telodendrimers as a nanodelivery tool and for supporting membrane proteins (61). The PEG^{5000}-CA_8 telodendrimer reagent was prepared according to methods published previously (42, 61). Small unilamellar vesicles of DMPC (Avanti Polar Lipids, Alabaster, AL) were prepared by probe sonication of a 20 mg/ml aqueous solution of DMPC until optical clarity was achieved; typically three intervals of 30 s were sufficient. After the sonication, the samples were centrifuged at 14,100 relative centrifugal force for 1 min to remove metal contamination from the probe tip. For the DMPC/PEG^{5000}-CA_8 mixtures, a total of 20 mg/ml DMPC and 2 mg/ml PEG^{5000}-CA_8 were mixed by pipetting at a volume ratio of 1:1.

Cell-free reaction

Small- and large-scale reactions (50 μl and 1 ml) were carried out using the RTS 500 ProteoMaster *E. coli* HY kit (Biotechrabbit GmbH, Hannover, Germany). Small-scale reactions contained the same ratio of components as the large-scale reactions. Reaction components (lysate, reaction mixture, feeding mixture, amino acid mixture, and methionine) were combined as specified by the manufacturer. For expression of mMOMP–tNLP, we added 0.3–1.5 μg of Δ49ApoA1 and 15 μg of mMOMP plasmid DNA to each 1-ml reaction. A total of 400 μl of DMPC/telodendrimer mixture was then added to the reaction mixture. The reactions were incubated at 30 °C with shaking at 300 rpm for 14–18 h in a floor shaker. The empty tNLPs were prepared using the same method but without the addition of the mMOMP plasmid.

Affinity purification of NLP-related complexes

Immobilized nickel affinity chromatography was used to isolate mMOMP–tNLP from the cell-free reaction mixture. 1 ml of a 50% slurry of cOmplete His-Tag Purification Resin (Roche Molecular Diagnostics) was equilibrated with equilibration buffer (50 mM NaH_2PO_4, 300 mM NaCl, pH 8.0) with 10 mM imidazole (Sigma-Aldrich) in a 10-ml chromatography column. The total cell-free reaction (1 ml) was mixed with the equilibrated resin and incubated/nutated at 4 °C for 1 h. The column was then washed with equilibration buffer containing 20 mM imidazole. The column was washed with 1 ml of the same buffer six times. The mMOMP–tNLPs were eluted in six 300-μl fractions of equilibration buffer containing 250 mM imidazole and one final elution of 300 μl in 500 mM imidazole. All elutions were analyzed by SDS-PAGE, and peak fractions containing protein were combined. Pooled fractions were dialyzed in PBS, pH 7.4, and then stored at 4 °C. All protein quantifications were done using a Qubit instrument according to the manufacturer's instructions (Thermo Fisher Scientific, Carlsbad, CA).

Material for mouse studies were tested for endotoxin levels using the Endosafe®-PTS™ (Charles River, Charleston, SC) endotoxin testing system based on the *Limulus* amebocyte lysate assay. All NLP preparations had an endotoxin level between 20 and 100 endotoxin units/mg.

SEC

NLPs were purified by SEC (Superdex 200, 3.2/300 GL column, GE Healthcare). SEC was run at a flow rate of 0.2 ml/min in PBS buffer with 0.25% PEG^{2000}.

SDS-PAGE

An aliquot of 5-15 μl of the eluted mMOMP–tNLPs were mixed with 4× NuPAGE lithium dodecyl sulfate sample buffer and 10× NuPAGE sample reducing agent (Life Technologies), heat-denatured, and loaded onto a 4–12% gradient premade 1.0 mM Bis-Tris gel (Life Technologies) along with the molecular weight standard SeeBlue Plus2 (Life Technologies). The running buffer was 1× MES-SDS (Life Technologies). Samples were run for 35 min at 200 V. Gels were stained with SYPRO Ruby protein gel stain (Life Technologies) according to the manufacturer's instructions and imaged using a LI-COR Odyssey Fc imager (LI-COR Biotechnology, Lincoln, NE). All protein bands were quantified using Image Studio V2.0 software (LI-COR Biosciences, Lincoln, NE) by densitometry.

Western blot and dot blot analyses

Western blotting and dot blotting were performed on PVDF membranes (Millipore). For Western blotting, samples were resolved with SDS-PAGE as described above. The gels were incubated in transfer buffer for 10 min and transferred at 4 °C for 65 min at 100V. The transfer buffer was 1× NuPAGE (Life Technologies). Blots were incubated overnight at 4 °C in Odyssey Blocking Buffer (PBS) (LI-COR Biotechnology) containing 0.2% Tween 20 and either 0.5 mg/ml mAb40 (linear, VD1) or 0.2 mg/ml Penta-His antibody (Qiagen, Hilden, Germany) diluted 1:1,000 for mAb40 and 1:500–1:1,000 for Penta-His (46). Blots were then washed for 5 min four times with PBS-T (50 mM NaH_2PO_4, 300 mM NaCl, 0.2% Tween 20, pH 7.4) while shaking. Blots were then incubated for 1 h in blocking buffer containing 0.2% Tween 20, 0.02% SDS, and 1 mg/ml IRDye 800CW goat (polyclonal) anti-mouse IgG (heavy and light) (LI-COR Biosciences) diluted to 1:10,000. Blots were washed with PBS-T four more times and imaged with a LI-COR Fc imager at 800 nm. All protein bands were quantified using Image Studio V2.0 software by densitometry.

For dot blotting, 3 μg of purified nanoparticles with and without mMOMP were blotted using the Bio-Dot apparatus (1706545, Bio-Rad) according to the manufacturer's instructions. Blots were developed as described above.

Conductance assays

To look at the ability of mMOMP to form functional pores, the mMOMP–tNLP complex was incorporated into a planar lipid bilayer, and conductance measurements were performed in a two-chamber black lipid membrane cell (Eastern Scientific LLC, Rockville, MD). A supported DMPC lipid bilayer was formed over a 200-μm-diameter aperture in a Teflon film partition using a painting technique. The *cis*-chamber (connected to a ground Ag/AgCl electrode) and *trans*-chamber (connected to a reference Ag/AgCl electrode) were filled with 0.2 and 2 ml

of PBS buffer (with Mg^{2+} and Ca^{2+}, pH 7.4), respectively. 1–2 μl of mMOMP–tNLP complex in solution was added to the *cis*-chamber above the DMPC bilayer. A holding potential between −100 and +100 mV was applied to the reference electrode, and the transmembrane current signal was recorded by an Axiopatch 200B patch clamp amplifier (Axon Instruments, Milpitas, CA) connected to a computer system running Clampex 10.3 software (Axon Instruments). The current traces were acquired at a sampling frequency of 10–100 kHz. The data were exported and analyzed using PClamp 10.3 software (Axon Instruments) and Igor Pro 6.31 (Wavemetrics Inc.).

DLS

Dynamic light scattering measurements of the NLP size were performed on a Zetasizer Nano ZS90 (Malvern Instruments, Malvern, UK) following the manufacturer's protocols. Each data point represents an average of at least 10 individual runs.

CryoEM

All tNLP and mMOMP–tNLP samples were preserved as frozen hydrated specimens in the presence of saturated ammonium molybdate for scanning with a JEOL JEM-2100F transmission electron microscope (JOEL USA, Peabody, MA) at magnification of 80,000× under liquid nitrogen temperature.

Mouse immune study

All animal studies were performed at the Lawrence Livermore National Laboratory in Public Health Service-assured facilities in accordance with guidelines set by the Animal Care and Use Committee. Female 3-week-old mice (BALB/c) were purchased from The Jackson Laboratory (Bar Harbor, ME). Because 3-week-old mice are prepubescent, they are more susceptible to STI infection and more suitable than adult mice for the *Chlamydia* studies. A total of six mice per group were vaccinated with the following formulations: 1×10^4 infectious units of *C. muridarum* EB obtained from Dr. Luis de la Maza at University of California, Irvine; 10 μg of tNLP with 5 μg of CpG adjuvant; 10 μg of mMOMP–tNLP plus 5 μg of CpG adjuvant; or PBS alone. Total volumes per inoculation were 50 μl. Animals were primed on day 1 and received boosts at days 21 and 42. Whole blood was drawn prior to each inoculation. A final bleed was conducted on day 61 post-initial prime.

Serum antigen-specific IgG antibody titers were measured using an enzyme-linked immunosorbent assay (ELISA). Immulon 2HB microtiter plates (Thermo Labsystems, Franklin, MA) were coated with the appropriate antigen (200 ng/well) and then incubated with sera (2-fold serial dilutions starting at 1:100 dilutions) for 1 h. Goat anti-mouse IgG HRP-conjugated antibody (KPL, Gaithersburg, MD) was added to the plates for 1 h, and the bound HRP was detected by incubation with tetramethylbenzidine (Sigma) quenched after 5 min with 1 M HCl. The reaction product was quantitated by a spectrophotometer at 450 nm, and values were corrected for background activity detected from wells that received diluent in place of sera. The titration curves were then fit to a power function in MS Office Excel, and titers were calculated from the fit function using a cutoff absorbance value of the average background OD ± 3 S.D.

Author contributions—M. A. C., T. C. P., N. O. F., C. D. B., A. N., A. R., H. G., and B. H. conceived and/or designed the experiments. M. A. C., C. D. B., W. H., M. F., A. C. E., J. G., D. H., F. B., N. O. F., L. X., and A. R. performed the experiments. W. H., M. A. C., A. C. E., J. G., F. B., N. O. F., A. N., R. H. C., A. R., and C. D. B. analyzed the data. K. S. L., K. K., N. W., Y. L., and B. H. contributed critical reagents/materials/analysis tools. W. H., A. C. E., N. O. F., A. N., A. R., and M. A. C. wrote the manuscript.

Acknowledgment—We thank Dr. Luis de la Maza for providing monoclonal antibodies, EB, and critical review of the manuscript.

References

1. Hafner, L. M., Wilson, D. P., and Timms, P. (2014) Development status and future prospects for a vaccine against *Chlamydia trachomatis* infection. *Vaccine* **32,** 1563–1571
2. Brunham, R. C., and Rey-Ladino, J. (2005) Immunology of *Chlamydia* infection: implications for a *Chlamydia trachomatis* vaccine. *Nat. Rev. Immunol.* **5,** 149–161
3. Schoborg, R. V. (2011) *Chlamydia* persistence—a tool to dissect *Chlamydia*–host interactions. *Microbes Infect.* **13,** 649–662
4. Thomson, N. R., and Clarke, I. N. (2010) *Chlamydia trachomatis*: small genome, big challenges. *Future Microbiol.* **5,** 555–561
5. Stratton, K. R., Durch, J. S., and Lawrence, R. S. (eds) (2000) *Vaccines for the 21st Century: a Tool for Decision Making*, pp. 362–364, National Academy Press, Washington, D. C.
6. Farris, C. M., Morrison, S. G., and Morrison, R. P. (2010) CD4+ T cells and antibody are required for optimal major outer membrane protein vaccine-induced immunity to *Chlamydia muridarum* genital infection. *Infect. Immun.* **78,** 4374–4383
7. Pal, S., Peterson, E. M., and de la Maza, L. M. (2005) Vaccination with the *Chlamydia trachomatis* major outer membrane protein can elicit an immune response as protective as that resulting from inoculation with live bacteria. *Infect. Immun.* **73,** 8153–8160
8. Pal, S., Theodor, I., Peterson, E. M., and de la Maza, L. M. (1997) Immunization with an acellular vaccine consisting of the outer membrane complex of *Chlamydia trachomatis* induces protection against a genital challenge. *Infect. Immun.* **65,** 3361–3369
9. Tifrea, D. F., Pal, S., Popot, J. L., Cocco, M. J., and de la Maza, L. M. (2014) Increased immunoaccessibility of MOMP epitopes in a vaccine formulated with amphipols may account for the very robust protection elicited against a vaginal challenge with *Chlamydia muridarum*. *J. Immunol.* **192,** 5201–5213
10. Findlay, H. E., McClafferty, H., and Ashley, R. H. (2005) Surface expression, single-channel analysis and membrane topology of recombinant *Chlamydia trachomatis* major outer membrane protein. *BMC Microbiol.* **5,** 5
11. Manning, D. S., and Stewart, S. J. (1993) Expression of the major outer membrane protein of *Chlamydia trachomatis* in *Escherichia coli*. *Infect. Immun.* **61,** 4093–4098
12. Sun, G., Pal, S., Weiland, J., Peterson, E. M., and de la Maza, L. M. (2009) Protection against an intranasal challenge by vaccines formulated with native and recombinant preparations of the *Chlamydia trachomatis* major outer membrane protein. *Vaccine* **27,** 5020–5025
13. Wen, Z., Boddicker, M. A., Kaufhold, R. M., Khandelwal, P., Durr, E., Qiu, P., Lucas, B. J., Nahas, D. D., Cook, J. C., Touch, S., Skinner, J. M., Espeseth, A. S., Przysiecki, C. T., and Zhang, L. (2016) Recombinant expression of *Chlamydia trachomatis* major outer membrane protein in *E. coli* outer membrane as a substrate for vaccine research. *BMC Microbiol.* **16,** 165
14. Takeda, H., Ogasawara, T., Ozawa, T., Muraguchi, A., Jih, P. J., Morishita, R., Uchigashima, M., Watanabe, M., Fujimoto, T., Iwasaki, T., Endo, Y., and Sawasaki, T. (2015) Production of monoclonal antibodies against GPCR using cell-free synthesized GPCR antigen and biotinylated liposome-based interaction assay. *Sci. Rep.* **5,** 11333

15. Kalmbach, R., Chizhov, I., Schumacher, M. C., Friedrich, T., Bamberg, E., and Engelhard, M. (2007) Functional cell-free synthesis of a seven helix membrane protein: *in situ* insertion of bacteriorhodopsin into liposomes. *J. Mol. Biol.* **371,** 639–648
16. Sonar, S., Patel, N., Fischer, W., and Rothschild, K. J. (1993) Cell-free synthesis, functional refolding, and spectroscopic characterization of bacteriorhodopsin, an integral membrane protein. *Biochemistry* **32,** 13777–13781
17. Chromy, B. A., Arroyo, E., Blanchette, C. D., Bench, G., Benner, H., Cappuccio, J. A., Coleman, M. A., Henderson, P. T., Hinz, A. K., Kuhn, E. A., Pesavento, J. B., Segelke, B. W., Sulchek, T. A., Tarasow, T., Walsworth, V. L., *et al.* (2007) Different apolipoproteins impact nanolipoprotein particle formation. *J. Am. Chem. Soc.* **129,** 14348–14354
18. Garda, H. A., Arrese, E. L., and Soulages, J. L. (2002) Structure of apolipophorin-III in discoidal lipoproteins. Interhelical distances in the lipid-bound state and conformational change upon binding to lipid. *J. Biol. Chem.* **277,** 19773–19782
19. Jonas, A. (1986) Reconstitution of high-density lipoproteins. *Methods Enzymol.* **128,** 553–582
20. Jonas, A., Sweeny, S. A., and Herbert, P. N. (1984) Discoidal complexes of A and C apolipoproteins with lipids and their reactions with lecithin: cholesterol acyltransferase. *J. Biol. Chem.* **259,** 6369–6375
21. Lu, B., Morrow, J. A., and Weisgraber, K. H. (2000) Conformational reorganization of the four-helix bundle of human apolipoprotein E in binding to phospholipid. *J. Biol. Chem.* **275,** 20775–20781
22. Blanchette, C. D., Cappuccio, J. A., Kuhn, E. A., Segelke, B. W., Benner, W. H., Chromy, B. A., Coleman, M. A., Bench, G., Hoeprich, P. D., and Sulchek, T. A. (2009) Atomic force microscopy differentiates discrete size distributions between membrane protein containing and empty nanolipoprotein particles. *Biochim. Biophys. Acta* **1788,** 724–731
23. Denisov, I. G., Grinkova, Y. V., Lazarides, A. A., and Sligar, S. G. (2004) Directed self-assembly of monodisperse phospholipid bilayer nanodiscs with controlled size. *J. Am. Chem. Soc.* **126,** 3477–3487
24. He, W., Luo, J., Bourguet, F., Xing, L., Yi, S. K., Gao, T., Blanchette, C., Henderson, P. T., Kuhn, E., Malfatti, M., Murphy, W. J., Cheng, R. H., Lam, K. S., and Coleman, M. A. (2013) Controlling the diameter, monodispersity, and solubility of ApoA1 nanolipoprotein particles using telodendrimer chemistry. *Protein Sci.* **22,** 1078–1086
25. Bhattacharya, P., Grimme, S., Ganesh, B., Gopisetty, A., Sheng, J. R., Martinez, O., Jayarama, S., Artinger, M., Meriggioli, M., and Prabhakar, B. S. (2010) Nanodisc-incorporated hemagglutinin provides protective immunity against influenza virus infection. *J. Virol.* **84,** 361–371
26. Bayburt, T. H., Grinkova, Y. V., and Sligar, S. G. (2006) Assembly of single bacteriorhodopsin trimers in bilayer nanodiscs. *Arch. Biochem. Biophys.* **450,** 215–222
27. Bayburt, T. H., Leitz, A. J., Xie, G., Oprian, D. D., and Sligar, S. G. (2007) Transducin activation by nanoscale lipid bilayers containing one and two rhodopsins. *J. Biol. Chem.* **282,** 14875–14881
28. Bayburt, T. H., and Sligar, S. G. (2003) Self-assembly of single integral membrane proteins into soluble nanoscale phospholipid bilayers. *Protein Sci.* **12,** 2476–2481
29. Cappuccio, J. A., Hinz, A. K., Kuhn, E. A., Fletcher, J. E., Arroyo, E. S., Henderson, P. T., Blanchette, C. D., Walsworth, V. L., Corzett, M. H., Law, R. J., Pesavento, J. B., Segelke, B. W., Sulchek, T. A., Chromy, B. A., Katzen, F., *et al.* (2009) Cell-free expression for nanolipoprotein particles: building a high-throughput membrane protein solubility platform. *Methods Mol. Biol.* **498,** 273–296
30. Frauenfeld, J., Gumbart, J., Sluis, E. O., Funes, S., Gartmann, M., Beatrix, B., Mielke, T., Berninghausen, O., Becker, T., Schulten, K., and Beckmann, R. (2011) Cryo-EM structure of the ribosome-SecYE complex in the membrane environment. *Nat. Struct. Mol. Biol.* **18,** 614–621
31. Gao, T., Blanchette, C. D., He, W., Bourguet, F., Ly, S., Katzen, F., Kudlicki, W. A., Henderson, P. T., Laurence, T. A., Huser, T., and Coleman, M. A. (2011) Characterizing diffusion dynamics of a membrane protein associated with nanolipoproteins using fluorescence correlation spectroscopy. *Protein Sci.* **20,** 437–447
32. Gao, T., Petrlova, J., He, W., Huser, T., Kudlick, W., Voss, J., and Coleman, M. A. (2012) Characterization of *de novo* synthesized GPCRs supported in nanolipoprotein discs. *PLoS One* **7,** e44911
33. Gogol, E. P., Akkaladevi, N., Szerszen, L., Mukherjee, S., Chollet-Hinton, L., Katayama, H., Pentelute, B. L., Collier, R. J., and Fisher, M. T. (2013) Three dimensional structure of the anthrax toxin translocon-lethal factor complex by cryo-electron microscopy. *Protein Sci.* **22,** 586–594
34. Leitz, A. J., Bayburt, T. H., Barnakov, A. N., Springer, B. A., and Sligar, S. G. (2006) Functional reconstitution of β2-adrenergic receptors utilizing self-assembling nanodisc technology. *BioTechniques* **40,** 601–602, 604, 606
35. Proverbio, D., Roos, C., Beyermann, M., Orbán, E., Dötsch, V., and Bernhard, F. (2013) Functional properties of cell-free expressed human endothelin A and endothelin B receptors in artificial membrane environments. *Biochim. Biophys. Acta* **1828,** 2182–2192
36. Sunahara, H., Urano, Y., Kojima, H., and Nagano, T. (2007) Design and synthesis of a library of BODIPY-based environmental polarity sensors utilizing photoinduced electron-transfer-controlled fluorescence ON/OFF switching. *J. Am. Chem. Soc.* **129,** 5597–5604
37. Blanchette, C. D., Fischer, N. O., Corzett, M., Bench, G., and Hoeprich, P. D. (2010) Kinetic analysis of his-tagged protein binding to nickel-chelating nanolipoprotein particles. *Bioconjug. Chem.* **21,** 1321–1330
38. Fischer, N. O., Blanchette, C. D., Chromy, B. A., Kuhn, E. A., Segelke, B. W., Corzett, M., Bench, G., Mason, P. W., and Hoeprich, P. D. (2009) Immobilization of His-tagged proteins on nickel-chelating nanolipoprotein particles. *Bioconjug. Chem.* **20,** 460–465
39. Fischer, N. O., Weilhammer, D. R., Dunkle, A., Thomas, C., Hwang, M., Corzett, M., Lychak, C., Mayer, W., Urbin, S., Collette, N., Chiun Chang, J., Loots, G. G., Rasley, A., and Blanchette, C. D. (2014) Evaluation of nanolipoprotein particles (NLPs) as an *in vivo* delivery platform. *PLoS One* **9,** e93342
40. Fischer, N. O., Rasley, A., Corzett, M., Hwang, M. H., Hoeprich, P. D., and Blanchette, C. D. (2013) Colocalized delivery of adjuvant and antigen using nanolipoprotein particles enhances the immune response to recombinant antigens. *J. Am. Chem. Soc.* **135,** 2044–2047
41. Weilhammer, D. R., Blanchette, C. D., Fischer, N. O., Alam, S., Loots, G. G., Corzett, M., Thomas, C., Lychak, C., Dunkle, A. D., Ruitenberg, J. J., Ghanekar, S. A., Sant, A. J., and Rasley, A. (2013) The use of nanolipoprotein particles to enhance the immunostimulatory properties of innate immune agonists against lethal influenza challenge. *Biomaterials* **34,** 10305–10318
42. Luo, J., Xiao, K., Li, Y., Lee, J. S., Shi, L., Tan, Y. H., Xing, L., Holland Cheng, R., Liu, G. Y., and Lam, K. S. (2010) Well-defined, size-tunable, multifunctional micelles for efficient paclitaxel delivery for cancer treatment. *Bioconjug. Chem.* **21,** 1216–1224
43. He, W., Scharadin, T. M., Saldana, M., Gellner, C., Hoang-Phou, S., Takanishi, C., Hura, G. L., Tainer, J. A., Carraway, K. L., 3rd, Henderson, P. T., and Coleman, M. A. (2015) Cell-free expression of functional receptor tyrosine kinases. *Sci. Rep.* **5,** 12896
44. Xu, X. P., Zhai, D., Kim, E., Swift, M., Reed, J. C., Volkmann, N., and Hanein, D. (2013) Three-dimensional structure of Bax-mediated pores in membrane bilayers. *Cell Death Dis.* **4,** e683
45. Sun, G., Pal, S., Sarcon, A. K., Kim, S., Sugawara, E., Nikaido, H., Cocco, M. J., Peterson, E. M., and de la Maza, L. M. (2007) Structural and functional analyses of the major outer membrane protein of *Chlamydia trachomatis*. *J. Bacteriol.* **189,** 6222–6235
46. Tifrea, D. F., Sun, G., Pal, S., Zardeneta, G., Cocco, M. J., Popot, J. L., and de la Maza, L. M. (2011) Amphipols stabilize the *Chlamydia* major outer membrane protein and enhance its protective ability as a vaccine. *Vaccine* **29,** 4623–4631
47. Haque, F., Geng, J., Montemagno, C., and Guo, P. (2013) Incorporation of a viral DNA-packaging motor channel in lipid bilayers for real-time, single-molecule sensing of chemicals and double-stranded DNA. *Nat. Protoc.* **8,** 373–392
48. Lai, G., Forti, K. M., and Renthal, R. (2015) Kinetics of lipid mixing between bicelles and nanolipoprotein particles. *Biophys. Chem.* **197,** 47–52
49. Carey, A. J., Cunningham, K. A., Hafner, L. M., Timms, P., and Beagley, K. W. (2009) Effects of inoculating dose on the kinetics of *Chlamydia*

muridarum genital infection in female mice. *Immunol. Cell Biol.* **87,** 337–343

50. Feher, V. A., Randall, A., Baldi, P., Bush, R. M., de la Maza, L. M., and Amaro, R. E. (2013) A 3-dimensional trimeric β-barrel model for *Chlamydia* MOMP contains conserved and novel elements of Gram-negative bacterial porins. *PLoS One* **8,** e68934
51. Kari, L., Whitmire, W. M., Crane, D. D., Reveneau, N., Carlson, J. H., Goheen, M. M., Peterson, E. M., Pal, S., de la Maza, L. M., and Caldwell, H. D. (2009) *Chlamydia trachomatis* native major outer membrane protein induces partial protection in nonhuman primates: implication for a trachoma transmission-blocking vaccine. *J. Immunol.* **182,** 8063–8070
52. Cappuccio, J. A., Blanchette, C. D., Sulchek, T. A., Arroyo, E. S., Kralj, J. M., Hinz, A. K., Kuhn, E. A., Chromy, B. A., Segelke, B. W., Rothschild, K. J., Fletcher, J. E., Katzen, F., Peterson, T. C., Kudlicki, W. A., Bench, G., *et al.* (2008) Cell-free co-expression of functional membrane proteins and apolipoprotein, forming soluble nanolipoprotein particles. *Mol. Cell. Proteomics* **7,** 2246–2253
53. Katzen, F., Fletcher, J. E., Yang, J. P., Kang, D., Peterson, T. C., Cappuccio, J. A., Blanchette, C. D., Sulchek, T., Chromy, B. A., Hoeprich, P. D., Coleman, M. A., and Kudlicki, W. (2008) Insertion of membrane proteins into discoidal membranes using a cell-free protein expression approach. *J. Proteome Res.* **7,** 3535–3542
54. Nikaido, H. (2003) Molecular basis of bacterial outer membrane permeability revisited. *Microbiol. Mol. Biol. Rev.* **67,** 593–656
55. Phale, P. S., Philippsen, A., Kiefhaber, T., Koebnik, R., Phale, V. P., Schirmer, T., and Rosenbusch, J. P. (1998) Stability of trimeric OmpF porin: the contributions of the latching loop L2. *Biochemistry* **37,** 15663–15670
56. Ferrara, L. G., Wallat, G. D., Moynié, L., Dhanasekar, N. N., Aliouane, S., Acosta-Gutiérrez, S., Pagès, J. M., Bolla, J. M., Winterhalter, M., Ceccarelli, M., and Naismith, J. H. (2016) MOMP from *Campylobacter jejuni* is a trimer of 18-stranded β-barrel monomers with a Ca^{2+} ion bound at the constriction zone. *J. Mol. Biol.* **428,** 4528–4543
57. Aistleitner, K., Heinz, C., Hörmann, A., Heinz, E., Montanaro, J., Schulz, F., Maier, E., Pichler, P., Benz, R., and Horn, M. (2013) Identification and characterization of a novel porin family highlights a major difference in the outer membrane of chlamydial symbionts and pathogens. *PLoS One* **8,** e55010
58. Gabay, J. E., Blake, M., Niles, W. D., and Horwitz, M. A. (1985) Purification of *Legionella pneumophila* major outer membrane protein and demonstration that it is a porin. *J. Bacteriol.* **162,** 85–91
59. Coleman M. A., Cappuccio, J. A., Blanchette, C. D., Gao, T., Arroyo, E. S., Hinz, A. K., Bourguet, F. A., Segelke, B., Hoeprich, P. D., Huser, T., Laurence, T. A., Motin, V. L., and Chromy, B. A. (2016) Expression and association of the *Yersinia pestis* translocon proteins, YopB and YopD, are facilitated by nanolipoprotein particles. *PLoS One* **11,** e0150166
60. Pal, S., Theodor, I., Peterson, E. M., and de la Maza, L. M. (2001) Immunization with the *Chlamydia trachomatis* mouse pneumonitis major outer membrane protein can elicit a protective immune response against a genital challenge. *Infect. Immun.* **69,** 6240–6247
61. Xiao, K., Suby, N., Li, Y., and Lam, K. S. (2013) Telodendrimer-based nanocarriers for the treatment of ovarian cancer. *Ther. Deliv.* **4,** 1279–1292